

Shortcuts to adiabaticity for an interacting Bose-Einstein condensate via exact solutions of the generalized Ermakov equation

Tang-You Huang,¹ Boris A. Malomed,^{2,3} and Xi Chen^{1,4, a)}

¹⁾*International Center of Quantum Artificial Intelligence for Science and Technology (QuArtist) and Department of Physics, Shanghai University, 200444 Shanghai, China*

²⁾*Department of Physical Electronics, School of Electrical Engineering, Faculty of Engineering, Tel Aviv University, P.O.B. 39040, Ramat Aviv, Tel Aviv, Israel*

³⁾*Center for Light-Matter Interaction, Tel Aviv University, P.O.B. 39040, Ramat Aviv, Tel Aviv, Israel*

⁴⁾*Department of Physical Chemistry, University of the Basque Country UPV/EHU, Apartado 644, 48080 Bilbao, Spain*

(Dated: 30 April 2020)

Shortcuts to adiabatic expansion of the effectively one-dimensional Bose-Einstein condensate (BEC) loaded in the harmonic-oscillator (HO) trap is investigated by combining techniques of the variational approximation and inverse engineering. Piecewise-constant (discontinuous) intermediate trap frequencies, similar to the known bang-bang forms in the optimal-control theory, are derived from an exact solution of a generalized Ermakov equation. Control schemes considered in the paper include imaginary trap frequencies at short time scales, i.e., the HO potential replaced by the quadratic repulsive one. Taking into regard the BEC's intrinsic nonlinearity, results are reported for the minimal transfer time, excitation energy (which measures deviation from the effective adiabaticity), and stability for the shortcut-to-adiabaticity protocols. These results are not only useful for the realization of fast frictionless cooling, but also help to address fundamental problems of the quantum speed limit and thermodynamics.

"Shortcuts to adiabaticity" (STA) for efficient transformation of trapped nonlinear-wave modes are important tools which help to improve quality of the transformation, simultaneously optimizing its efficiency. In this work, we focus on the shortcuts for expansion of effectively one-dimensional Bose-Einstein condensates (BECs), described by the Gross-Pitaevskii equation (GPE) including the cubic self-interaction of the wave function and the harmonic-oscillator (HO) trapping potential with a time-dependent strength. We design simple but fast STA protocols, using the method of inverse engineering, realized by means of the variational approximation applied to the GPE. A generalized Ermakov equation, including an additional term induced by the self-interaction of the BEC, is thus derived (the classical second-order ordinary differential equation of this type was derived and solved by Russian mathematician Ermakov about 150 years ago). Results of the analysis help us to elaborate schemes for the time modulation of the HO-trap frequency, admitting fast frictionless cooling of the expanding BEC in the weak-interaction regime. In particular, the schemes based on the "bang" and "bang-bang" forms, which are well known in the optimal-control theory, are exemplified. The minimal transformation time, time-averaged energy of excitations generated around the expanding state, and stability of the dynamical regimes with attractive and repulsive self-interactions are analyzed for various STA protocols. In addition to direct applications to the expansion (or compression) of BEC, the results are relevant for studies of the quantum speed limit and manifestations of the third principle of thermodynamics in quantum systems in general.

I. INTRODUCTION

Precise control and manipulations of non-interacting and interacting Bose-Einstein condensates (BECs) in trapping potentials has well-known significance to applications ranging from quantum simulations, information processing, and quantum-enhanced metrology to atom interferometry¹. A particularly relevant example is the transfer a quantum system from the ground state of one potential into that of another, through its evolution governed by a specifically designed Hamiltonian. To this end, slow adiabatic processes², as well as fast shortcuts through intermediate states³, Fourier transform⁴, optimal control⁵⁻⁷, and machine learning⁸ have been exploited for the realization of fast frictionless cooling and transport of cold atoms, trapped ions, and BEC in magneto-optical traps, and high-quality compression of optical solitons³.

As concerns the concept of "shortcuts to adiabaticity" (STA), it has recently drawn much interest to speed up slow adiabatic processes, while suppressing the excitation or heating, with important applications to atomic, molecular, optical and statistical physics, see reviews⁹⁻¹¹. In this context, a series of works were devoted to frictionless expansion/compression and cooling of atomic Bose-Einstein condensates (BECs) in time-modulated harmonic-oscillator (HO) traps¹²⁻¹⁷, with extensions to cold-atom mixtures¹⁸, Tonks-Girardeau (TG)^{19,20} and Fermi^{21,22} gases, and many-body systems^{23,24}. These results are not only significant for the design of optimal quantum control^{25,26}, but also have significant implications for the studies of quantum speed limits, in the context of the trade-off between time and energy cost under the constraint of the

^{a)}Electronic mail: xchen@shu.edu.cn

third law in quantum thermodynamics^{27,28}. Other systems, such as mechanical resonators²⁹, photonic lattices³⁰, bosonic Josephson junction³¹⁻³⁴, Brownian particles³⁵ and classical RC circuits³⁶ have been extensively studied by using similar STA techniques for the swift transformation between two adiabatic or equilibrium states.

Theoretically, the STA techniques, among which the most popular ones are inverse engineering¹³, counter-diabatic driving^{20,37,38} and fast-forward scaling^{39,40}, which were elaborated in different setups, although they are mathematically equivalent^{40,41}. In the contexts of the inverse engineering, Lewis-Riesenfeld dynamical invariant¹³, or general scaling transformations^{42,43}, various forms of the famous Ermakov equation⁴⁴⁻⁴⁹ were derived for designing shortcuts to adiabatic expansions of non-interacting thermal gases and BEC in the Thomas-Fermi (TF) regime^{12,15-17}. Specifically, when it comes to the shortcuts for BECs, the TF regime^{12,17} or time-dependent nonlinear coupling¹² lead to (modified) Ermakov equations, starting from the Gross-Pitaevskii (GP) equation, which is the commonly adopted dynamical model of BEC in the mean-field theory⁵⁰.

In this work, inspired by approaches based on the variational approximation (VA)^{51,52}, similar to those developed in nonlinear optics^{3,53}, we derive a generalized Ermakov equation, including a term induced by the self-interaction term in the GP equation. The objective is to further elaborate shortcuts for the adiabatic expansion/compression in BEC. This allows us to manipulate nonlinear dynamics of BEC solitons by means of the Feshbach resonance^{54,55} and many-body dynamics in power-law potentials⁵⁶. In particular, we exploit the VA to design shortcuts to adiabaticity for the decompression of BEC in HO traps. Exact solutions to the generalized Ermakov equation, including bang and bang-bang control scenarios, are analytically obtained and used to highlight the effect of interatomic interactions on the minimal time and stability of the BEC manipulations. The results for the time-optimal driving are different from those previously obtained for single atoms^{25,26,28} and BEC in the TF limit⁵⁷, where negligible or very strong interactions are assumed.

II. THE MODEL, HAMILTONIAN, AND VARIATIONAL APPROACH

We begin with the effective one-dimensional (1D) GP equation, modeling the mean-field dynamics of the cigar-shaped BEC⁵⁸:

$$i\frac{\partial\psi}{\partial t} = -\frac{1}{2}\frac{\partial^2\psi}{\partial x^2} + \frac{1}{2}\omega^2(t)x^2\psi + gN|\psi|^2\psi, \quad (1)$$

where $\omega(t)$ is time-dependent trapping frequency, g is the nonlinearity coefficient representing atom-atom interaction, and N is the total number of atoms. The scaled variables are related to their counterparts measured in physical units (with tildes) as per $t = \omega_0\tilde{t}$, $\omega(t) = \tilde{\omega}(t)/\omega_0$, $x = \tilde{x}/\sigma_0$, $g = \tilde{g}/\hbar\omega_0\sigma_0$, where m is atomic mass, ω_0 is the initial longitudinal trapping frequency, $\sigma_0 = \sqrt{\hbar/m\omega_0}$ is the corresponding cloud size, $\tilde{g} = 2\hbar a_s\omega_\perp$ with scattering length a_s and the

trapping frequency of the transverse potential, ω_\perp , which provides for reduction of the underlying three-dimensional GP equation to the 1D form (1), provided that ω_\perp is much larger than the one acting in the axial direction. Further, if the axial HO potential is time-dependent, the use of the 1D equation (1) is fully justified if the respective frequencies of the time dependence are much smaller than ω_\perp .

In order to apply the VA^{51,52}, we start with the Lagrangian density of Eq. (1),

$$\mathcal{L} = \frac{i}{2}\left(\psi\frac{\partial\psi^*}{\partial t} - \psi^*\frac{\partial\psi}{\partial t}\right) - \frac{1}{2}\left|\frac{\partial\psi}{\partial x}\right|^2 - \frac{1}{2}\omega^2(t)x^2|\psi|^2 - \frac{1}{2}gN|\psi|^4. \quad (2)$$

Plugging the usual time-dependent Gaussian ansatz,

$$\psi(x,t) = A(t)\exp\left[-\frac{x^2}{2a^2(t)} + ib(t)x^2\right], \quad (3)$$

in Eq. (2), we calculate the effective Lagrangian $L = \int_{-\infty}^{+\infty}\mathcal{L}[\psi]dx$. Here $a(t)$ and $b(t)$ represent the width and chirp of the wave function, and amplitude $A(t) = (1/\pi a^2)^{1/4}$ is the amplitude of wave function, determined by the normalization condition, $\int_{-\infty}^{+\infty}|\psi(x)|^2dx = 1$. The variational procedure applied to the Lagrangian makes it possible to eliminate the chirp, $b = -\dot{a}/2a$, the resulting Euler-Lagrange equation for $a(t)$ taking the form of the generalized Ermakov equation⁵⁹:

$$\ddot{a} + \omega^2(t)a = \frac{1}{a^3} + \frac{gN}{\sqrt{2\pi}a^2}, \quad (4)$$

which is tantamount to the Newton's equation of motion for a particle with unit mass, $\ddot{a} = -dU(a)/da$ (with the overdot standing for the time derivative), with the effective potential and the corresponding energy,

$$U(a) = \frac{1}{2}\omega^2(t)a^2 + \frac{1}{2a^2} + \frac{gN}{\sqrt{2\pi}a}, \quad (5)$$

$$\mathcal{E}(a) = \frac{\dot{a}^2}{2} + \frac{1}{2}\omega^2(t)a^2 + \frac{1}{2a^2} + \frac{gN}{\sqrt{2\pi}a}. \quad (6)$$

The presence of term $\sim gN$ in Eq. (4) makes it different from the original Ermakov equation,

$$\ddot{a} + \omega^2(t)a = \frac{1}{a^3}, \quad (7)$$

derived from the Lewis-Riesenfeld invariant¹³ or by means of the scaling transform^{42,43}, see also Appendix A.

III. SHORTCUTS TO ADIABATICITY

In this section, we aim to construct STA protocols of time-dependent trapping by selecting an appropriate time-dependent frequency in Eq. (4), to guarantee a fast transform from the ground state at time $t = 0$ to another ground state at a fixed final time, $t = t_f$, avoiding additional (unwanted)

excitations. The initial value is taken as $\omega(0) = 1$, and the final one is defined as $\omega(t_f) = 1/\gamma^2$, i.e., $\gamma \equiv \sqrt{\omega_0/\omega_f}$ may be considered an appropriate control parameter. To guarantee that the initial and final states are stationary ones, one has to impose the following boundary conditions:

$$a(0) = a_i, \quad a(t_f) = a_f, \quad (8)$$

$$\dot{a}(0) = \dot{a}(t_f) = 0, \quad (9)$$

$$\ddot{a}(0) = \ddot{a}(t_f) = 0, \quad (10)$$

where a_i and a_f are unique positive real solutions of equations

$$a_i^4 - \frac{gN}{\sqrt{2\pi}} a_i = 1, \quad (11)$$

$$\frac{a_f^4}{\gamma^4} - \frac{gN}{\sqrt{2\pi}} a_f = 1, \quad (12)$$

which follow from the generalized Ermakov equation (4) with $\ddot{a}(0) = \ddot{a}(t_f) = 0$. Clearly, $a_i = 1$ and $a_f = \gamma$ in the limit $gN \rightarrow 0$. Therefore, by analogy to the perturbative Kepler problem, the boundary conditions defined by Eqs. (8)-(10) imply minimization of the effective potential $U(a)$ (5), as well as of the energy given by Eq. (6) without the kinetic-energy term.

A. Inverse engineering

Here we address an example of atomic cooling by decompressing from initial frequency $\omega_0 = 250 \times 2\pi$ Hz to the final one $\omega_f = 2.5 \times 2\pi$ Hz. In the linear limit, $gN \rightarrow 0$, the values are $a_i = 1$ and $a_f = \gamma = 10$. However, due to the atom-atom interaction, the initial and final sizes of the BEC cloud are slightly different, $a_i = 1.001$ and $a_f = 10.099$, as calculated numerically from Eqs. (11) and (12) with the nonlinearity strength gN . The boundary conditions being fixed, trajectory of $a(t)$ may be approximated by the simplest polynomial ansatz¹³,

$$a(t) = a_i - 6(a_i - a_f)s^5 + 15(a_i - a_f)s^4 - 10(a_i - a_f)s^3, \quad (13)$$

with $s = t/t_f$. As a consequence, smooth function $\omega(t)$ may be *inversely determined* by Eq. (4). If an imaginary trap frequency is dealt with, which corresponds to a parabolic repeller, instead of the HO trap, in Eq. (1), t_f may be formally made arbitrarily short. However, physical constraints always exist in practice, see the discussion below. Generally, the use of the switch between the trapping and expulsive potentials extends possibilities for the design of control schemes with diverse functionalities.

Here we chose $t_f = 5.45$, such that the absolute value of the real frequency is bounded by ω_0 ($\omega_0 < \omega_f$). Figure 1 illustrates the respective time-varying trap frequency and evolution of the width, as produced by the inverse-engineering method, where the initial and final trap frequencies are $\omega(0) = 1$ and $\omega(t_f) = 1/\gamma^2$, and $gN = 0.01$. Later, we will compare such smooth trajectories with results produced by the so-called bang and bang-bang control, which is relevant for the time-optimal solution, implemented by means of piecewise-constant (discontinuous) intermediate trap frequencies.

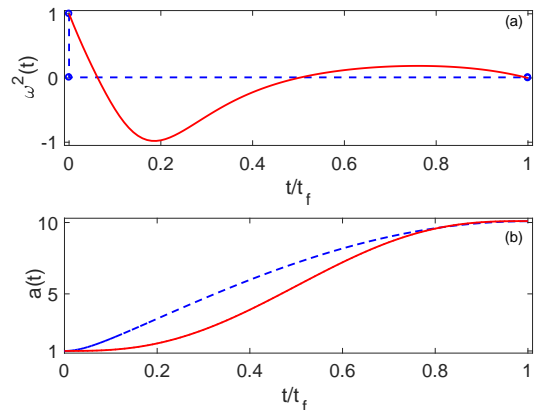


FIG. 1. The time dependence of the designed trap frequency, $\omega(t)$ (a), and width of the wave packet (b). Red solid and blue dashed lines correspond to the inverse engineering and bang control, respectively. The parameters are $\omega(0) = 1$, $\omega(t_f) = 1/\gamma^2$, $gN = 0.01$. Note that $t_f = 5.45$ for the inverse engineering is different $t_f = 15.83$ for 2-jump control.

B. The two-jump control

In the limit of $gN \rightarrow 0$, a simple exact solution of the Ermakov equation can be constructed, that reproduces the shortcut with just one intermediate frequency²⁸, similar to the scenario for the compression of solitons in nonlinear fibers, by passing the soliton from a fiber segment with a large dispersion coefficient to a segment with a smaller one. This scenario was theoretically elaborated in Ref.³ and experimentally realized in⁶⁰. Motivated by this, we assume that, at $t = 0$, the trap frequency suddenly changes from $\omega(0)$ to some constant intermediate value ω_c , to achieve an alternative shortcut.

In the linear limit, $gN \rightarrow 0$, the trap frequency remains equal to ω_c , from $t = 0$ to

$$t_f = \pi / (2\omega_c), \quad (14)$$

and at moment $t = t_f$ the frequency instantaneously changes from ω_c to the final value, $\omega(t_f)$. The exact solution of the Ermakov equation (7) with constant ω_c is well known:

$$a^2(t) = \frac{1}{2} [(A + C) + (A - C) \cos(2\omega_c t)], \quad (15)$$

with constants A and C subject to constraint $AC = 1/\omega_c^2$. To secure the transformation of a stationary state taken at $t = 0$ into another stationary one at $t = t_f$, it is necessary to impose the above-mentioned conditions, $a(0) = 1$, $a(t_f) = \gamma$, and $\dot{a}(0) = \dot{a}(t_f) = 0$. After a straightforward algebra, the combination of such conditions and Eq. (15) yields a simple solution:

$$a(t) = \sqrt{1 + \frac{1 - \omega_c^2}{\omega_c^2} \sinh^2(\omega_c t)}, \quad (16)$$

with

$$\omega_c = \sqrt{\omega(0)\omega(t_f)} = 1/\gamma. \quad (17)$$

Thus, Eqs. (14) and (16) provide a simple exact solution for the shortcut if the nonlinearity is negligible. In particular, the necessary intermediate trapping frequency ω_c is given as the geometric mean of the initial and final frequencies.

The solution can be generalized for full equation (4), although in a less explicit form. The shortcut scenario implies that the initial and final values (8), subject to boundary conditions (9), are coupled by the motion in potential (5). The energy conservation in this mechanical (perturbative Kepler) problem implies $U(a_i) = U(a_f)$, or, in an explicit form,

$$\omega_c^2 = \frac{1}{a_i^2 a_f^2} + \sqrt{\frac{2}{\pi}} \frac{gN}{a_i a_f (a_i + a_f)}. \quad (18)$$

In this case, a simple expression for t_f is not available, but it can be written in the form of an integral:

$$t_f = \int_{a_i}^{a_f} \frac{da}{\sqrt{2[U(a_{\text{in}}) - U(a)]}}, \quad (19)$$

where a_i and a_f are given by Eq. (8). Thus, the trap frequency $\omega(t)$ and trajectory for $a(t)$ can be obtained in a numerical form from Eq. (4) with boundary conditions, see Fig. 1, where $\omega_c = 0.0993$ and $t_f = 15.83$ are obtained for the chosen parameters, $\omega(0) = 1$, $\omega(t_f) = 1/\gamma^2$, and $gN = 0.01$. Most importantly, the designed trajectory $a(t)$ satisfies the boundary conditions (8) and (9), which guarantees the realization of the STA protocol and secures the stability at $t > t_f$. However, since the boundary condition (10), for the second derivative of $a(t)$, is not fulfilled, one has to design the trap frequency suddenly change. Namely, the trap frequency has to “jump” from initial value ω_0 to intermediate one ω_c at $t = 0$, and “jump” back to final one ω_f at $t = t_f$.

C. The three-jump bang-bang control

Next, we address the generalized Ermakov equation (4) and discuss the time-minimization optimal-control problem with a constrained trap frequency, that is, $|\omega(t)|^2 \leq \delta$. To follow the usual conventions adopted in the optimal control theory, we set new notation,

$$x_1 \equiv a, \quad x_2 \equiv \dot{a}, \quad (20)$$

$u(t) \equiv \omega^2(t)$, and rewrite Eq. (4) as a system of the first-order differential equations:

$$\dot{x}_1 = x_2, \quad (21)$$

$$\dot{x}_2 = -ux_1 + \frac{1}{x_1^3} + \frac{gN}{\sqrt{2\pi}} \frac{1}{x_1^2}, \quad (22)$$

where x_1, x_2 are the components of a “state vector” \mathbf{x} , and squared trap frequency $u(t)$ is considered as a (scalar) control function. The form of the theoretical time-optimal solution can be found using the Pontryagin’s maximum principle, which provides necessary conditions for the optimality. Similar to the approach used in Refs.^{26,57}, determining the optimal frequency profile reduces to finding $u(t)$ subject to the bound

$|u(t)| \leq \delta$ with $u(0) = 1$ and $u(t_f) = 1/\gamma^2$, such that the above system starts with initial conditions $(x_1(0), x_2(0)) = (a_i, 0)$, and reaches the final point $(x_1(t_f), x_2(t_f)) = (a_f, 0)$ in minimal time t_f . The boundary conditions for x_1 and x_2 may be equivalently considered as those for a and \dot{a} , see Eqs. (8) and (9). The boundary conditions for $u(t)$ are equivalent to those for $\omega(t)$ and, through Eq. (4) or Eqs. (11) and (12), equivalent to those for \ddot{a} , hence there are, totally, six boundary conditions, as in Eqs. (8-10).

To find the minimal time t_f , we define the cost function,

$$J = \int_0^{t_f} dt = t_f. \quad (23)$$

The control Hamiltonian $H_c(\mathbf{p}, \mathbf{x}, u)$ is

$$H_c(\mathbf{p}, \mathbf{x}, u) = p_0 + p_1 x_2 - p_2 x_1 u + \frac{p_2}{x_1^3} + \frac{gN}{\sqrt{2\pi}} \frac{p_2}{x_1^2}, \quad (24)$$

where vector $\mathbf{p} = (p_0, p_1, p_2)$ is composed of non-zero and continuous Lagrange multipliers, $p_0 < 0$ may be chosen for convenience, as it amounts to multiplying the cost function by a constant, and $p_{1,2}$ obey the Hamilton’s equations: $\dot{\mathbf{x}} = \partial H_c / \partial \mathbf{p}$ and $\dot{\mathbf{p}} = -\partial H_c / \partial \mathbf{x}$. For almost all $0 \leq t \leq t_f$, function $H_c(\mathbf{p}, \mathbf{x}, u)$ attains its maximum at $u = u(t)$, and $H_c(\mathbf{p}, \mathbf{x}, u)$ is a constant. Making use of the Hamiltonian’s equation, we arrive at the following explicit expressions:

$$\dot{p}_1 = p_2 \left(u + \frac{3}{x_1^4} + \frac{2gN}{\sqrt{2\pi}} \frac{1}{x_1^3} \right), \quad (25)$$

$$\dot{p}_2 = -p_1. \quad (26)$$

It is clear that the control Hamiltonian $H_c(\mathbf{p}, \mathbf{x}, u)$ is a linear function of variable $u(t)$. Therefore, the maximization of $H_c(\mathbf{p}, \mathbf{x}, u)$ is determined by the sign of term $-up_2 x_1$, which, in turn, is determined by the sign of p_2 , as $a(t)$ is always positive, i.e., $x_1 > 0$ and $p_2 \neq 0$. Here $p_2 = 0$ does not provide singular control, and only takes place at specific moments (switching times). As a consequence, we arrive at the scheme of the “bang-bang” control, defined by the following form:

$$u(t) = \begin{cases} -\delta, & p_2 > 0, \\ \delta, & p_2 < 0, \end{cases} \quad (27)$$

which implies that the controller switches from one boundary value to the other at the switching times. When u is constant and Eq. (4) holds, then it can be derived that

$$x_2^2 + ux_1^2 + \frac{1}{x_1^2} + \frac{2gN}{\sqrt{2\pi}x_1} = c, \quad (28)$$

where c is an integration constant. Moreover, we see from Eq. (6) that trajectories with constant u correspond to constant energy $\mathcal{E}(a) = c/2$.

By choosing the simplest but feasible “bang-bang” control with only one intermediate switching at $t = t_1$, we introduce the three-jumps form,

$$u(t) = \begin{cases} 1 & t = 0, \\ -\delta, & 0 < t < t_1, \\ \delta, & t_1 < t < t_2, \\ 1/\gamma^2 & t = t_f = t_1 + t_2, \end{cases} \quad (29)$$

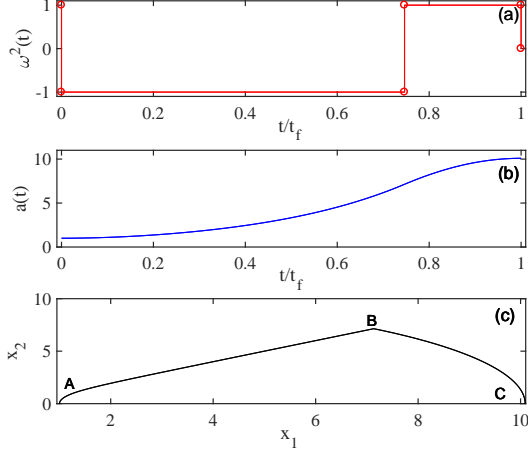


FIG. 2. Controller u for “bang-bang” scheme with one intermediate switch (a), the width a of the wave packet (b), and the corresponding trajectory (c). Parameters: $\delta = 1$ and others are the same as those in Fig. 1.

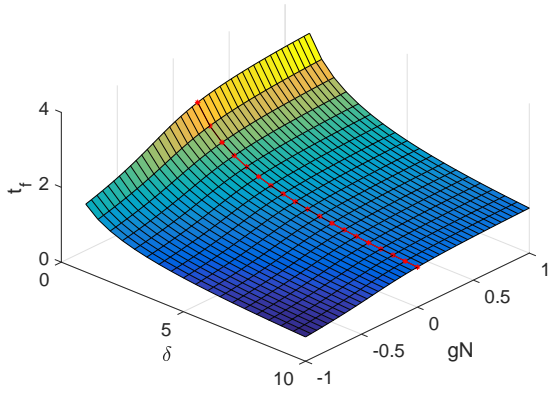


FIG. 3. The dependence of minimal time t_f on bound δ of the trap frequency and nonlinearity gN , other parameters being the same as in Fig. 1. The red dashed line indicates the minimal time predicted by the optimal-control theory for $gN = 0$.

as shown in Fig. 2(a), where we take $\delta = 1$ as an example, and other parameters are the same as in Fig. 1. Obviously, the discontinuities at the time edges are not implied by the maximum principle, but are determined by the initial and final conditions imposed on control u . This guarantees the creation of the STA protocol, but requires the sudden change of the trap frequencies. Therefore, we can find a lower bound on the minimum time, achieved only with instantaneous jumps of the control at the initial and final times.

Next, we aim to calculate the necessary time for the transfer from the initial point, $A(a_i, 0)$, to the final one, $C(a_f, 0)$, as shown in Fig. 2(c), where $B(x_1^B, x_2^B)$ is the intermediate point at the switching instant, $t = t_1$. With the control function taken as per Eq. (29), and boundary conditions (8-10), we obtain

segment AB:

$$\dot{x}_1^2 - \delta x_1^2 + \frac{1}{x_1^2} + \frac{2gN}{\sqrt{2\pi}x_1} = c_1, \quad (30)$$

with $c_1 \equiv -\delta a_i^2 + 1/a_i^2 + 2gN/\sqrt{2\pi}a_i$, and segment BC:

$$\dot{x}_1^2 + \delta x_1^2 + \frac{1}{x_1^2} + \frac{2gN}{\sqrt{2\pi}x_1} = c_2, \quad (31)$$

with $c_2 \equiv \delta a_f^2 + 1/a_f^2 + 2gN/\sqrt{2\pi}a_f$. By using Eqs. (30) and (31), the continuity condition at $t = t_1$ can be resolved for x_1^B as follows:

$$x_1^B = \sqrt{\frac{1}{2}(a_f^2 + a_i^2) + \frac{(a_i^2 - a_f^2)}{2\delta a_i^2 a_f^2} + \frac{gN(a_i - a_f)}{\sqrt{2\pi}\delta a_i a_f}}. \quad (32)$$

Once the intermediate point x_1^B at switching time $t = t_1$ is determined, we finally obtain

$$t_f = t_1 + t_2, \quad (33)$$

where

$$t_1 = \int_{a_i}^{x_1^B} \frac{dx}{\sqrt{\delta x^2 - 1/x^2 + gN/\sqrt{2\pi}x + c_1}}, \quad (34)$$

$$t_2 = \int_{x_1^B}^{a_f} \frac{dx}{\sqrt{-\delta x^2 - 1/x^2 + gN/\sqrt{2\pi}x + c_2}}, \quad (35)$$

Figures 2(b) and (c) illustrate the evolution of the soliton’s width and trajectory in phase space (x_1, x_2) , corresponding to controller $u(t)$ of the “bang-bang” type, where the parameters are $\omega(0) = 1$, $\omega(t_f) = 1/\gamma^2$, $gN = 0.01$ and $\delta = 1$. In this manner, we can find the minimal time for atomic cooling, $t_f = 3.097$, which is slightly larger than minimal time $t_f = 3.088$ ^{26,27}, obtained when in the linear limit, $gN = 0$. In the opposite TF limit, the minimal time $t_f = 3.809$ is still large, see a detailed calculation in Appendix A. Of course, it may be possible to analyze the control strategy for schemes with additional intermediate switchings, to predict shorter time for desired transfer.

Figure 3 shows the dependence of minimal time t_f for the “bang-bang” control on the trap-frequency bound δ and nonlinearity strength gN . On the one hand, the minimal time approaches zero if there is no bound, i.e., $\delta \rightarrow \infty$. On the other hand, minimal time t_f is essentially affected by the nonlinearity. The minimal time for the expansion of the condensate trapped in the time-varying potential decreases with the increase of the nonlinearity strength (through the Feshbach resonance). For instance, the minimal time $t_f = 3.079$ for $gN = -0.01$ is somewhat smaller than $t_f = 3.088$ for $gN = 0$, as indicated by the pointed line in Fig. 3. Thus, the self-attractive (repulsive) nonlinearity accelerates the expansion (compression) of the condensate. Furthermore, when gN takes larger values, BEC enters the TG regime. In this case, the scaling transformation leads to the ordinary Ermakov equation, the minimal time taking the above-mentioned value $t_f = 3.088$, as the dynamics of the TG gas can be reduced to a

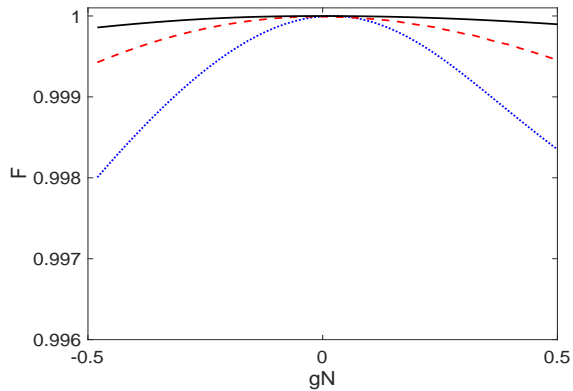


FIG. 4. The dependence of the fidelity, defined as per Eq. (36) on nonlinearity strength gN , with the initial and final wave functions calculated by means of the imaginary-time evolution method. The state evolution, produced by different STA protocols, including inverse engineering (black solid), two-jump bang (blue dotted), and three-jump bang-bang (red dashed) schemes, is simulated with the help of the split-step method. Parameters are the same as those in Figs. 1 and 2.

single-particle evolution, by dint of the Bose-Fermi mapping. However, the system's fidelity and stability become quite different when gN changes from positive to negative values, as shown below.

IV. DISCUSSION

A. Stability

Here we aim to explore stability of different STA protocols, designed on the basis of the inverse engineering, two-jump and three-jump bang-bang schemes, against the variation of the nonlinearity strength gN . To this end, we calculate the fidelity defined as

$$F = |\langle \tilde{\psi}_f(x) | \psi(x, t_f) \rangle|^2, \quad (36)$$

where wave function $|\tilde{\psi}_f\rangle$ is the final stationary state. Here the imaginary-time evolution method is used for obtaining the initial and final stationary states, and the state evolving along the shortcut trajectory is numerically calculated by means of the split-step method. As illustrated by Fig. 4, the smooth STA trajectory designed by dint of inverse engineering demonstrates, in general, better tolerance against the nonlinearity effects (which make the fidelity poorer), as two or three-jump protocols require abrupt changes of the frequency to satisfy the boundary conditions, which is a challenging condition. The STA protocols are more stable for $gN > 0$ than for the opposite sign, as the Newtonian particle can easier escape from the effective potential well when the nonlinearity is self-attractive. As a matter of fact, the nonlinearity strongly affects the initial and final sizes of the BEC cloud (8). Under the action of weak nonlinearity, the difference between stationary states produced by the imaginary-time evolution method and

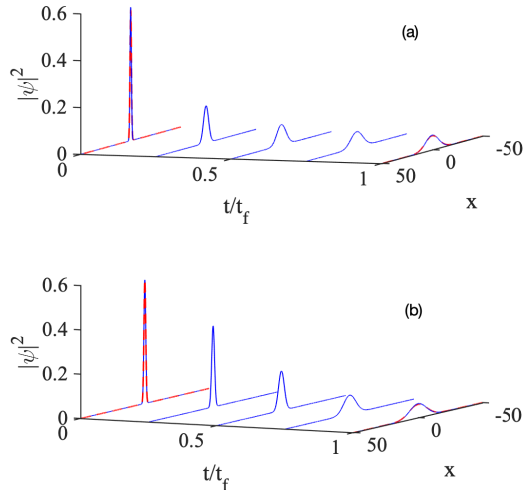


FIG. 5. The evolution of the particle density (squared absolute value of the wave function) governed by the GP equation (1), with trap frequency $\omega(t)$ modulated in time by (a) the two-jump (17) and (b) the three-jump bang-bang (29) controls. Red dashed lines represent the initial and final particle densities calculated as per the variational approximation. They are virtually indistinguishable from the counterparts produced by the numerical solution of the GP equation. Parameters are the same as those in Fig. 2.

the assumed Gaussian wave packets with initial and final values of a [see Eq. (3)] is negligible. Furthermore, Fig. 5 shows the time evolution of the particle density, produced by the numerical solution of the time-dependent GP equation (1), and its counterpart predicted by the VA (dashed red curves). The figure corroborates the validity of the VA based on Gaussian ansatz (13), while the trap frequency changes abruptly at the switching points.

Apart from that, the implementation of our proposed protocols in realistic BEC experiments requires careful considerations. First, one has to apply two pinch coils to offset a purely magnetic Ioffe-Pritchard trap, thus producing an expulsive quadratic potential, instead of the HO one⁶¹. An alternative way for achieving the same purpose is to combine a time-dependent red-detuned optical dipole trap with an additional blue-detuned antitrap¹³. Second, sudden changes of on-off controller entail the fast trap modulation, which might lead to unwanted intrinsic excitation of the state under the consideration⁶². To avoid this, a multiple shooting method should be used for smoothing the bang-bang control scheme⁶³. It is also important to mention that our idealized model amounts to an effectively 1D trap, produced by integrating the underlying three-dimensional GP equation in the transverse directions, under the action of the confinement in the transverse plane⁵⁸. The use of magnetic and optical traps allows one to independently control of the axial and transverse frequencies. In fact, the radial-longitudinal coupling in the 3D setting sets a limit for the time scale on which the 1D equation is valid. It may be improved by increasing the waist of the

trapping laser beam⁶⁴. To be more precise, by taking into account longitudinal anharmonic perturbations, the lower validity bound for the ground-state decompression in the Gaussian trap is found to be $t_f \gg 3\hbar/8mw^2\omega_f^2$ ^{13,65}, with m and w being the mass of Rb⁸⁷ atoms and the laser-beam's waist. Thus, after choosing the initial and final frequencies, we obtain $t_f \gg 0.7$ for $w = 50 \mu\text{m}$ and $t_f \gg 0.08$ for $w = 150 \mu\text{m}$, showing the validity of different STA protocols with high fidelity under realistic conditions.

B. Excitation energy

The STA protocols support the frictionless cooling subject to the initial and final boundary conditions. However, the process itself is not adiabatic at all, thus excitation of the system on top of the stationary state may lead to detrimental effects. To address this issue, we define the time-average energy as

$$\bar{\mathcal{E}} = \frac{1}{t_f} \int_0^{t_f} \mathcal{E}(t) dt. \quad (37)$$

Substituting Eq. (6), and integrating once with the use of boundary conditions (8)-(10), we obtain

$$\bar{\mathcal{E}} = \frac{1}{t_f} \int_0^{t_f} \left(\dot{a}^2 + \frac{1}{a^2} + \frac{3gN}{2\sqrt{2\pi}a} \right) dt. \quad (38)$$

The dependence of the so computed excitation energy on the nonlinearity strength is presented in Fig. 5. In principle, such an energy price of STA protocols is stipulated by the time-energy uncertainty, which implies increase of the (time-averaged) energy for shorter times. It is seen that the two-jump bang scheme produces smaller excitation energy, as the corresponding operation time is larger. With the same frequency bound, the operation time for the inverse-engineering scheme is larger than for the time-optimal bang-bang one, which leads to a smaller excitation energy as well. One can use another ansatz for the inverse engineering to minimize the excitation energy, as discussed in work²⁸. In addition, we point out that, as the bang and bang-bang schemes require sudden jumps to match the boundary conditions, the extra energy cost has to be paid at the edges, to fully implement these schemes.

Finally, we note that the STA approach for atom cooling has fundamental implications for the third law of thermodynamics, with the atoms being the medium in a quantum refrigerator. Figure 7 quantifies the third law in this case, i.e., the minimal time diverges when the final trap frequency ω_f , proportional to temperature, approaches zero. In a more general case, we see from Fig. 7 that the unattainability principle is quantified as

$$t_f \propto \log(a_f) + \frac{\pi}{4}, \quad (39)$$

where a_f is a positive real solution of Eq. (12), and we keep the first two terms of its Taylor's expansion around $gN = 0$,

$$a_f = \left(\frac{\omega_0}{\omega_f} \right)^{1/2} + \frac{gN}{4\sqrt{2\pi}} \left(\frac{\omega_0}{\omega_f} \right)^{3/2} + O^2(gN). \quad (40)$$

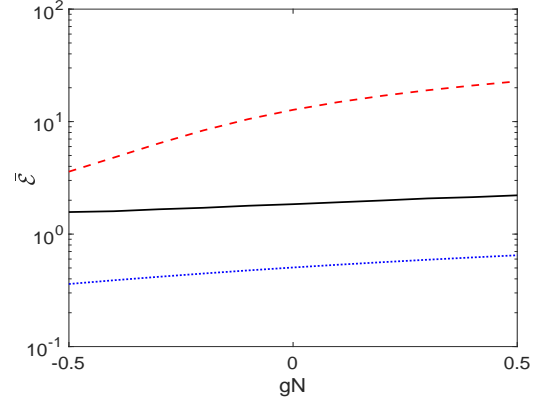


FIG. 6. The dependence of time-average energy $\bar{\mathcal{E}}$, defined by Eq. (37), on the nonlinearity strength gN , for the inverse-engineering (black solid), two-jump bang (blue dotted), and three-jump bang-bang (red dashed) schemes. Parameters are the same as in Figs. 1 and 2.

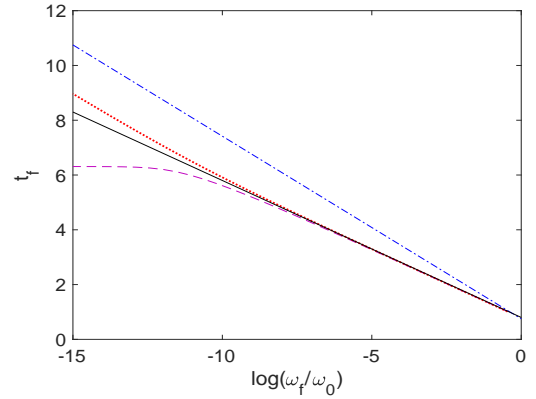


FIG. 7. The minimum time for bang-bang scheme, as a function of $\log(\omega_f/\omega_0)$: the TF limit (the dashed-dotted blue line), $gN = 0$ (the solid black line), $gN = 0.01$ (the dotted red line), and $gN = -0.01$ (the dashed purple line), other parameters being the same as in Fig. 2.

Interestingly, from Eq. (40) we recover the scaling law, $t_f \propto (\omega_0/\omega_f)^{1/2}$, when $gN = 0$, leading to the cooling rate, $R \propto T^{3/2}$, of the quantum refrigerator^{7,27,28}. In the TF limit, the second term in Eq. (40) becomes dominant, yielding $t_f \propto (\omega_0/\omega_f)^{3/2}$, with the corresponding cooling rate $R \propto T^2$. Remarkably, the self-repulsive nonlinearity provides a larger exponent, therefore the repulsive interaction, acting in the course of the cooling process, may improve the cooling rate. When the nonlinear Feshbach heat engine⁵⁵ is considered, the attractive self-interaction implies the shorter time, leading to the improvement of the work. But in this case the stability is weaker, and the collapse of the wave packet exists at $\omega_f \ll 1$.

V. CONCLUSION

To summarize, we have discussed the STA (shortcut to adiabaticity) for the expansion of weakly interacting BEC loaded in the HO (harmonic-oscillator) trap. The analysis is based on the use of the generalized Ermakov equation, derived from the VA (variational approximation) applied to the effective 1D Gorss-Pitaevskii equation. Exact solutions of the generalized Ermakov equation are *inverse engineered* to design smooth or piecewise-constant intermediate time dependences of the trap frequency, which realize the STA schemes. In particular, we focused on the minimal transition time and the minimization of the excitation energy produced by STA. To this end, the time-optimal solutions provided by the bang-bang scheme with a smooth polynomial ansatz, and by the two-jump bang scheme, have been compared. We conclude that the self-attractive nonlinearity in BEC can help to shorten the minimal time. The latter result which may have fundamental implications for the consideration of the quantum speed limit and third law of thermodynamics in quantum systems.

Finally, we point out several pending issues to be addressed. The stability with respect to the intrinsic BEC nonlinearity is reasonable, but the validity of the VA derivation of the Ermakov equation is predicated upon the accuracy of the Gaussian ansatz. Definitely, the bright soliton based on the hyperbolic-tangent function may be another option. Another noteworthy point is that the time-optimal solution has been obtained by means of the “bang-bang” scheme. It requires the sudden change of the trap frequency, that may be difficult to implement physically. One can further optimize the trajectory with more constraints imposed on the first, or even second, derivatives of the time dependence of the trap frequency. An alternative may be to use a smooth ansatz with polynomial and trigonometric functions for constructing the time-optimal “bang-bang” scheme, as discussed in Ref.⁶⁶. All these results may apply to analyzing the transport, splitting, and compression of solitons^{54,55}, and also to various anharmonic potentials^{56,65}, e.g. with quadratic terms.

ACKNOWLEDGMENTS

We acknowledge support from National Natural Science Foundation of China (NSFC) (11474193), STCSM (2019SHZDZX01-ZX04, 18010500400 and 18ZR1415500), Program for Eastern Scholar, Ramón y Cajal program of the Spanish MCIU (RYC-2017-22482), QMiCS (820505) and OpenSuperQ (820363) of the EU Flagship on Quantum Technologies, Spanish Government PGC2018- 095113-B-I00 (MCIU/AEI/FEDER, UE), Basque Government IT986-16, as well as the and EU FET Open Grant Quomorphic. The work of BAM is supported, in part, by the Israel Science Foundation, through grant No. 1286/17.

DATA AVAILABILITY STATEMENT

The data that support the findings of this study are available from the corresponding author upon reasonable request.

- ¹C. Cohen-Tannoudji and D. Guéry-Odelin, *Advances in atomic physics: an overview* (World Scientific, 2011).
- ²A. Kastberg, W. D. Phillips, S. L. Rolston, R. J. C. Spreeuw, and P. S. Jessen, *Phys. Rev. Lett.* **74**, 1542 (1995).
- ³D. Anderson, M. Lisak, B. Malomed, and M. Quiroga-Teixeiro, *JOSA B* **11**, 2380 (1994).
- ⁴A. Couvert, T. Kawalec, G. Reinaudi, and D. Guéry-Odelin, *EPL (Europhysics Letters)* **83**, 13001 (2008).
- ⁵A. Bulatov, B. Vugmeister, A. Burin, and H. Rabitz, *Phys. Rev. A* **58**, 1346 (1998).
- ⁶A. Bulatov, B. E. Vugmeister, and H. Rabitz, *Phys. Rev. A* **60**, 4875 (1999).
- ⁷P. Salamon, K. H. Hoffmann, Y. Rezek, and R. Kosloff, *Physical Chemistry Chemical Physics* **11**, 1027 (2009).
- ⁸B. M. Henson, D. K. Shin, K. F. Thomas, J. A. Ross, M. R. Hush, S. S. Hodgman, and A. G. Truscott, *Proceedings of the National Academy of Sciences* **115**, 13216 (2018).
- ⁹E. Torrontegui, S. Ibáñez, S. Martínez-Garaot, M. Modugno, A. del Campo, D. Guéry-Odelin, A. Ruschhaupt, X. Chen, and J. G. Muga, in *Advances in atomic, molecular, and optical physics*, Vol. 62 (Elsevier, 2013) pp. 117–169.
- ¹⁰D. Guéry-Odelin, A. Ruschhaupt, A. Kiely, E. Torrontegui, S. Martínez-Garaot, and J. G. Muga, *Rev. Mod. Phys.* **91**, 045001 (2019).
- ¹¹A. del Campo and K. Kim, *New Journal of Physics* **21**, 050201 (2019).
- ¹²J. Muga, X. Chen, A. Ruschhaupt, and D. Guéry-Odelin, *Journal of Physics B: Atomic, Molecular and Optical Physics* **42**, 241001 (2009).
- ¹³X. Chen, A. Ruschhaupt, S. Schmidt, A. del Campo, D. Guéry-Odelin, and J. G. Muga, *Phys. Rev. Lett.* **104**, 063002 (2010).
- ¹⁴J.-F. Schaff, X.-L. Song, P. Vignolo, and G. Labeyrie, *Phys. Rev. A* **82**, 033430 (2010).
- ¹⁵J.-F. Schaff, X.-L. Song, P. Capuzzi, P. Vignolo, and G. Labeyrie, *EPL (Europhysics Letters)* **93**, 23001 (2011).
- ¹⁶A. Del Campo, *EPL (Europhysics Letters)* **96**, 60005 (2011).
- ¹⁷J.-F. Schaff, P. Capuzzi, G. Labeyrie, and P. Vignolo, *New Journal of Physics* **13**, 113017 (2011).
- ¹⁸S. Choi, R. Onofrio, and B. Sundaram, *Phys. Rev. A* **84**, 051601 (2011).
- ¹⁹A. del Campo, *Phys. Rev. A* **84**, 031606 (2011).
- ²⁰S. Deffner, C. Jarzynski, and A. del Campo, *Phys. Rev. X* **4**, 021013 (2014).
- ²¹D. J. Papoular and S. Stringari, *Phys. Rev. Lett.* **115**, 025302 (2015).
- ²²S. Deng, P. Diao, Q. Yu, A. del Campo, and H. Wu, *Phys. Rev. A* **97**, 013628 (2018).
- ²³D. Guéry-Odelin, J. G. Muga, M. J. Ruiz-Montero, and E. Trizac, *Phys. Rev. Lett.* **112**, 180602 (2014).
- ²⁴W. Rohringer, D. Fischer, F. Steiner, I. E. Mazets, J. Schmiedmayer, and M. Trupke, *Scientific reports* **5**, 9820 (2015).
- ²⁵Y. Rezek, P. Salamon, K. H. Hoffmann, and R. Kosloff, *EPL (Europhysics Letters)* **85**, 30008 (2009).
- ²⁶D. Stefanatos, J. Ruths, and J.-S. Li, *Phys. Rev. A* **82**, 063422 (2010).
- ²⁷K. Hoffmann, P. Salamon, Y. Rezek, and R. Kosloff, *EPL (Europhysics Letters)* **96**, 60015 (2011).
- ²⁸X. Chen and J. G. Muga, *Phys. Rev. A* **82**, 053403 (2010).
- ²⁹Y. Li, L.-A. Wu, and Z. D. Wang, *Phys. Rev. A* **83**, 043804 (2011).
- ³⁰D. Stefanatos, *Phys. Rev. A* **90**, 023811 (2014).
- ³¹B. Juliá-Díaz, E. Torrontegui, J. Martorell, J. G. Muga, and A. Polls, *Phys. Rev. A* **86**, 063623 (2012).
- ³²A. Yuste, B. Juliá-Díaz, E. Torrontegui, J. Martorell, J. G. Muga, and A. Polls, *Phys. Rev. A* **88**, 043647 (2013).
- ³³D. Stefanatos and E. Paspalakis, *New Journal of Physics* **20**, 055009 (2018).
- ³⁴T. Hatomura, *New Journal of Physics* **20**, 015010 (2018).
- ³⁵I. A. Martínez, A. Petrosyan, D. Guéry-Odelin, E. Trizac, and S. Ciliberto, *Nature physics* **12**, 843 (2016).
- ³⁶S. Faure, S. Ciliberto, E. Trizac, and D. Guéry-Odelin, *American Journal of Physics* **87**, 125 (2019).
- ³⁷M. V. Berry, *Journal of Physics A: Mathematical and Theoretical* **42**, 365303 (2009).

- ³⁸A. del Campo, *Phys. Rev. Lett.* **111**, 100502 (2013).
³⁹S. Masuda and K. Nakamura, *Phys. Rev. A* **78**, 062108 (2008).
⁴⁰E. Torrontegui, S. Martínez-Garaot, A. Ruschhaupt, and J. G. Muga, *Phys. Rev. A* **86**, 013601 (2012).
⁴¹X. Chen, E. Torrontegui, and J. G. Muga, *Phys. Rev. A* **83**, 062116 (2011).
⁴²Y. Castin and R. Dum, *Phys. Rev. Lett.* **77**, 5315 (1996).
⁴³V. Gritsev, P. Barmettler, and E. Demler, *New Journal of Physics* **12**, 113005 (2010).
⁴⁴V. P. Ermakov, *Izv. Univ. Kiev (in Russian)* **20**, 1 (1880).
⁴⁵H. R. Lewis, *Phys. Rev. Lett.* **18**, 510 (1967).
⁴⁶J. L. Reid and J. R. Ray, *Journal of Mathematical Physics* **21**, 1583 (1980).
⁴⁷J. R. Ray, *Physics Letters A* **78**, 4 (1980).
⁴⁸C. Rogers and W. K. Schief, *Ermakov-type systems in nonlinear physics and continuum mechanics*, In: N. Euler, editor, *Nonlinear systems and their remarkable mathematical structures*, (CRC Press, 2018) pp. 541–576.
⁴⁹W. S. C. Rogers and B. Malomed, *Comm. Nonlin. Sci. Num. Sim.*, 105091 (2020).
⁵⁰L. P. Pitaevskii and S. Stringari, *Bose–Einstein Condensation* (Oxford University Press, Oxford, 2003).
⁵¹V. M. Pérez-García, H. Michinel, J. I. Cirac, M. Lewenstein, and P. Zoller, *Phys. Rev. Lett.* **77**, 5320 (1996).
⁵²J. J. García-Ripoll, V. M. Pérez-García, and P. Torres, *Phys. Rev. Lett.* **83**, 1715 (1999).
⁵³B. A. Malomed, *Progress in optics* **43**, 71 (2002).
⁵⁴J. Li, K. Sun, and X. Chen, *Sci. Rep.* **6**, 38258 (2016).
⁵⁵J. Li, T. Fogarty, S. Campbell, X. Chen, and Th. Busch, *New J. Phys.* **20**, 015005 (2018).
⁵⁶T.-N. Xu, J. Li, T. Busch, X. Chen, and T. Fogarty, *Phys. Rev. Research* (2020).
⁵⁷D. Stefanatos and J.-S. Li, *Phys. Rev. A* **86**, 063602 (2012).
⁵⁸L. Salasnich, A. Parola, and L. Reatto, *Phys. Rev. A* **65**, 043614 (2002).
⁵⁹E. Quinn and M. Haque, *Phys. Rev. A* **90**, 053609 (2014).
⁶⁰A. Barak, O. Peleg, C. Stucchio, A. Soffer, and M. Segev, *Phys. Rev. Lett.* **100**, 153901 (2008).
⁶¹L. Khaykovich, F. Schreck, G. Ferrari, T. Bourdel, J. Cubizolles, L. D. Carr, Y. Castin, and C. Salomon, *Science* **296**, 1290 (2002).
⁶²L. D. Carr and Y. Castin, *Phys. Rev. A* **66**, 063602 (2002).
⁶³M. H. X. C. Yongcheng Ding, Tangyou Huang, [arXiv:2002.11605](https://arxiv.org/abs/2002.11605).
⁶⁴E. Torrontegui, X. Chen, M. Modugno, A. Ruschhaupt, D. Guéry-Odelin, and J. G. Muga, *Phys. Rev. A* **85**, 033605 (2012).
⁶⁵X.-J. Lu, X. Chen, J. Alonso, and J. G. Muga, *Phys. Rev. A* **89**, 023627 (2014).
⁶⁶V. Martikyan, D. Guéry-Odelin, and D. Sugny, *Phys. Rev. A* **101**, 013423 (2020).

Appendix A

In the appendix, we first present an alternative way to derive the minimal time in TF limit for the consistence and further comparison. We use a set of equations for the density, n , and phase gradient, $\nabla\phi(x,t)$, of the wave function, represented in the Madelung form,

$$\psi(x,t) = \sqrt{n(x,t)}e^{i\phi(x,t)}. \quad (\text{A1})$$

Thus, the continuity equation derived from the GP equation (1) is

$$\frac{\partial n(x,t)}{\partial t} + \nabla \cdot (n \mathbf{v}) = 0, \quad (\text{A2})$$

where the velocity of the superflow is defined by

$$\mathbf{v} = \frac{1}{2i} \frac{(\psi^* \nabla \psi - \psi \nabla \psi^*)}{|\psi|^2} \equiv \nabla \phi. \quad (\text{A3})$$

Next, we insert expression (A1) in Eq. (1), the real part of which yielding the Euler equation:

$$\frac{\partial \mathbf{v}}{\partial t} = -\nabla \left[-\frac{1}{2} \frac{\nabla^2 \sqrt{n}}{\sqrt{n}} + \frac{\mathbf{v}^2}{2} + \frac{1}{2} \omega^2(t)x^2 + gn \right]. \quad (\text{A4})$$

In the case of the strongly self-repulsive condensate, the TF approximation⁵⁰ allows one to omit the kinetic-energy term in Eq. (A4) (the first term of right-hand side), thus neglecting the quantum pressure, the result being

$$\frac{\partial \mathbf{v}}{\partial t} + \frac{\partial}{\partial x} \left(\frac{\mathbf{v}^2}{2} + \frac{1}{2} \omega^2(t)x^2 + gn \right) = 0 \quad (\text{A5})$$

In the TF approximation, the initial equilibrium density distribution is $n_0(x,t) = (\mu - \omega^2(0)x^2/2)/g$, according to the time-independent GP equation with chemical potential μ . The scaling approach to the hydrodynamic equation is commonly used to study dynamical properties of cold atomic system. It is based on ansatz of $n(x,t) = n_0[x/a(t)]/a(t)$, which satisfies the initial condition $n(x,0) = n_0(x)$ and $a(0) = 1$. Then, one obtains the velocity field from the continuity equation (A2):

$$\mathbf{v} = \frac{\dot{a}(t)}{a(t)}x \quad (\text{A6})$$

Combining the TF limit and the scaling approach by inserting expression (A6) in Eq. (A5) produces the evolution equation for scaling factor $a(t)$:

$$\ddot{a} + \omega^2(t)a = \frac{\omega_0^2}{a^2}. \quad (\text{A7})$$

Next, we need to transfer the initial ground state from trap frequency $\omega(0) = 1$ at $t = 0$ to the target state with $\omega(t_f) = 1/\gamma^2$. And the same boundary conditions, Eqs. (8-10), where $a_i = 1$ and $a_f = \gamma^{4/3}$, are imposed to guarantee the realization of STA. Then, in terms of notation (20), the dynamical equations are rewritten as

$$\dot{x}_1 = x_2, \quad (\text{A8})$$

$$\dot{x}_2 = -\tilde{u}x_1 + \frac{1}{x_1^2}, \quad (\text{A9})$$

where the control function $\tilde{u}(t) \equiv \omega^2(t)/\omega_0^2$ is used, subject to the bound $|\tilde{u}(t)| \leq \delta$, and variables $x_{1,2}$ satisfies obey the constraint

$$x_2^2 + \tilde{u}x_1^2 + \frac{2}{x_1} = c, \quad (\text{A10})$$

where c is an integration constant. The time-optimal solution of the ‘‘bang-bang’’ type⁵⁷ for $\tilde{u}(t)$ is built as the same as $u(t)$ in (29). Applying the calculations similar to those presented in Eqs. (30)–(33), the expressions for the duration of these two segments reads

$$t_1 = \int_{a_i}^{a_f} \frac{dx_1}{\sqrt{\delta x_1^2 - 2/x_1 + c}}, \quad (\text{A11})$$

$$t_2 = \int_{x_1^B}^{a_f} \frac{dx_1}{\sqrt{-\delta x_1^2 - 2/x_1 + c_2}}, \quad (\text{A12})$$

with $c_1 = 2/a_i - \delta a_i^2$ and $c_2 = \delta a_f^2 + 2/a_f$. The intermediate switching point x_1^B is found as

$$x_1^B = \sqrt{\frac{a_f^2 + a_i^2}{2} + \frac{a_i - a_f}{\delta a_i a_f}}. \quad (\text{A13})$$

The minimum time in the TF limit, t_f , is now $t_f = t_1 + t_2$.

Finally, we briefly present the time-optimal scheme for the ordinary Ermakov equation (7). In this case, the boundary conditions, Eqs. (8-10), hold with $a_i = 1$ and $a_f = 1/\gamma$. Following Ref.²⁶, the minimal time $t_f = t_1 + t_2$ is obtained, where the switching times t_1 and t_2 are

$$t_1 = \frac{1}{\sqrt{\delta}} \sinh^{-1} \sqrt{\frac{(\gamma^2 - 1)(\gamma^2 \delta - 1)}{2\gamma^2(1 + \delta)}}, \quad (\text{A14})$$

$$t_2 = \frac{1}{\sqrt{\delta}} \sin^{-1} \sqrt{\frac{(\gamma^2 - 1)(\gamma^2 \delta + 1)}{2(\gamma^4 \delta - 1)}}. \quad (\text{A15})$$

By setting $\delta = 1$, we eventually obtain

$$t_1 = -\frac{1}{r^2} \log \left(\frac{\omega_0}{\omega_f} \right), \quad (\text{A16})$$

$$t_2 = \pi/4, \quad (\text{A17})$$

as indicated in Fig. 7.